The association of native T1 mapping and reduced myocardial strain in patients with end stage renal disease on hemodialysis. Non-invasive assessment of myocardial fibrosis.

Matthew PM Graham-Brown[1,2,3], Daniel S March[1,2], Darren R Churchward[1,2], David J Stensel[3], Anvesha Singh[4], Ranjit Arnold[4], James O Burton[1,2,4], Gerry P McCann[4]

[1]John Walls Renal Unit, University Hospitals Leicester NHS Trust, UK
[2] Department of Infection Immunity and Inflammation, School of Medicine and Biological Sciences, University of Leicester, UK
[3]National Centre for Sport and Exercise Medicine, School of Sport, Exercise and Health Sciences, Loughborough University, UK
[4]Dept of Cardiovascular Sciences, University of Leicester and NIHR Leicester Cardiovascular Biomedical Research Unit, Glenfield Hospital Leicester

Correspondence address: Dr MPM Graham-Brown
Department of Infection, Immunity and Inflammation,
University of Leicester, Leicester, LE1 9HN, UK.
Telephone: +44 (0)116252 2522
Fax: +44 (0)116 252 5111
Email: mpmgb1@le.ac.uk

Acknowledgments: This study is independent research arising from a Clinician Scientist Award (Dr James Burton, CS-2013-13-014) supported by the NIHR, an NIHR grant to Gerald McCann (NIHR-CDF 2014-07-045) and a grant from the Van Geest Foundation. This work is also supported by the NIHR Leicester Cardiovascular Biomedical Research Unit based at University Hospitals of Leicester and the University of Leicester and the NIHR Diet, Lifestyle & Physical Activity Biomedical Research Unit based at University Hospitals of Leicester and Loughborough University.
The views expressed in this publication are those of the authors and not necessarily those of the National Health Service, the National Institute for Health Research or the Department of Health.

Running Title: T1 mapping & strain in HD patients

Abstract word count: 235

Manuscript word count: 3632

Abstract

Left ventricular hypertrophy and myocardial fibrosis frequently occur in patients with end stage renal disease on hemodialysis and are associated with poor prognosis. Native T1 mapping is a novel cardiac MRI (CMR) technique that measures native myocardial T1 relaxation, a surrogate of myocardial fibrosis. We assessed the relationship between CMR measured native T1 mapping and cardiac function. We compared global and segmental native myocardial T1 time and global longitudinal, circumferential and segmental strain of hemodialysis patients (n=35) and controls (n=22). Native global T1 time was significantly higher in the hemodialysis group than the control group (1269.51ms (1241.72-1289.01) vs 1085.2ms (1066-1109.2), $P<0.001$), with the septal regions of hemodialysis patients having significantly higher T1 times than non-septal regions (1292.7ms (1258.9-1310.4) vs 1252.3 (1219.2-1269.6), $P=0.002$). Peak global circumferential and global longitudinal strain were significantly reduced in hemodialysis patients compared to controls (GCS -18.3 ± 3.3% vs -21.7 ± 3.1% and GLS -16.1 ± 3.3% vs -20.4 ± 2.6%, both P<0.001). Systolic strain was also reduced in the septum compared to non-septal myocardium in HD patients (-16.2±4.6 vs -21.9±3.9, P<0.001) but not in controls. Global circumferential and longitudinal strain correlated with global native T1 values (r=0.41, P=0.002, r=0.55, P<0.001) and septal native T1 correlated with septal systolic strain (r=0.46, P<0.001). These results suggest that myocardial fibrosis may be assessed non-invasively with T1 mapping and that the interventricular septum is particularly prone to the development of fibrosis in hemodialysis patients.

Key Words: Native T1, Hemodialysis, Strain, Fibrosis, Cardiorenal, MRI

Introduction

Post-mortem and biopsy studies have demonstrated that patients with chronic kidney disease (CKD), and end stage renal disease (ESRD) on hemodialysis (HD) have high levels of interstitial myocardial fibrosis (1,2). This pattern of fibrosis is greater in HD patients than in patients with milder CKD and is progressively more severe with increasing dialysis vintage (1). Interstitial fibrosis progresses over time to irreversible replacement fibrosis (2) (overt myocardial scarring) and fibrosis does not fully reverse in patients who receive renal transplantation, with levels of interstitial fibrosis similar to that seen in patients with dilated cardiomyopathy (2). The pathogenesis of myocardial fibrosis in HD patients is complex. Myocardial hypertrophy and subsequent ischemia result in cellular apoptosis (3) and autophagic signals that lead to activation of pathways that increase production of extracellular matrix (4-6). Increasing levels of myocardial fibrosis lead to ventricular stiffening and consequent diastolic and systolic dysfunction that may ultimately lead to the congestive cardiac failure or dilated cardiomyopathy (7). Myocardial fibrosis in HD patients has been shown to be highly arrhythmogenic, and contributes to the high incidence of sudden cardiac death in this patient group (5,6,8,9). Extensive myocardial fibrosis has also been shown to be a stronger predictor of death than myocyte hypertrophy in HD patients (2).

Whilst LV ejection fraction (EF) is an important measure of cardiac function it is well known that its prognostic value in HD patients is limited when in the normal range (10). As in other cardiac diseases, myocardial dysfunction is likely to be directly impaired in the presence of diffuse fibrosis (11,12). Subtle, subclinical impairment of cardiac systolic function may be detected by assessing myocardial systolic strain, which measures myocardial deformation (13). CMR studies have shown that global myocardial strain is reduced in patients with CKD (14,15) and ESRD (16).

Previously there has been no reliable way of tracking the development and progression of myocardial fibrosis non-invasively. Gadolinium enhanced cardiac MRI (CMR) is frequently used to detect replacement myocardial fibrosis in other

populations. However, gadolinium based contrast agents (GBAs) can no longer be used in HD patients (17) due to the rare, but serious complication of nephrogenic systemic fibrosis (NSF) (18). Native T1 mapping is a novel non-contrast CMR technique that enhances tissue characterization with CMR, correlating well with biopsy measured myocardial fibrosis in aortic stenosis (19,20) and can differentiate patients with hypertrophic cardiomyopathy from hypertensive cardiac disease (21). Native T1 mapping therefore offers a potential method of quantifying myocardial fibrosis (both diffuse interstitial and replacement myocardial fibrosis) in patients with advanced CKD, and patients with ESRD on dialysis, without the need for gadolinium based contrast agents (22).

We hypothesized that native T1 time would be increased and be associated with impaired myocardial strain in HD patients compared to controls.

Results

35 HD and 22 control patients were included in the study. Demographic data of both groups are shown in table 1. Cine CMR image quality was good (n=27) or excellent (n=30) allowing quantitation of LV volumes, mass and strain in all patients. For segmental analysis of T1, in the HD patients, 5 out of 210 segments were not analyzable due to artefact, and in the control patients, 3 out of 132 segments were not analyzable.

Volumes and masses

LV mass and volumes were significantly increased and EF was reduced in HD patients compared to controls, although the median EF of HD group was within the normal range (table 2). Mass/volume was not different between groups. Ten patients in the HD group had an EF below 50% (range 36-49.1%).

Systolic strain

Global circumferential strain (GCS) and global longitudinal strain (GLS) were significantly reduced in HD patients compared to controls (Table 2). When only HD patients with an EF greater than 50% were included (n=25) GCS and GLS both remained significantly impaired compared to controls (figure 1). Mid-ventricular circumferential systolic strain was significantly reduced in the septal compared to non-septal segments in HD patients (figure 2). Two-way ANOVA showed that there was a significant main effects of group (P<0.001), segment (P<0.001) and group*segment interaction (P =0.008). Sidak's multiple comparison tests showed a significant difference between septal and non-septal regions in HD patients (P<0.001; figure 2), confirming mid-ventricular circumferential systolic strain was significantly reduced in the septal region of HD patients compared to non-septal region and to controls. No significant difference between septal and non-septal segments was seen in the mid-ventricular slice of the control group (figure 2).

Visual assessment of native T1 maps

Visual assessment of the native T1 parametric maps was undertaken to look for areas of focal increased signal that likely indicate replacement fibrosis (23,24). Of the 35 native T1 maps in the HD group, 17 were assessed as having areas of discretely increased signal, with the predominant areas being inferior RV

insertion point hyperintensity (n=11), septal (n=10) and or inferior wall (n=6) mid-wall hyperintensity and anterior mid-wall hyperintensity (n=3). In the control group only 4 out of 22 subjects had inferior insertion point hyperintensity and only one patient had septal mid-wall increased signal. Fishers exact test confirmed there was a significant difference between HD and controls groups for areas of discrete mid-wall or insertion point hyperintensity (*P*=0.026). Figure 3 shows the mid-ventricular end-diastolic cine MRI and native T1 maps of 1 control and 3 HD patients with progressively increasing native T1 times (23).

Native T1 mapping in HD vs. Control group

Median native global T1 signal was significantly higher in the HD group compared to the controls (Table 2). Native T1 was significantly higher in the septal compared to non-septal segments in HD patients (figure 4). Two-way ANOVA showed there was a significant main effect of group (*P*<0.001), segment (*P*=0.005) and group*segment interaction effect (*P* =0.005). Sidak's multiple comparison tests showed a significant difference between septal and non-septal regions in HD patients (*P*<0.001; figure 4) confirming T1 signal was significantly higher in the septal region of HD patients compared non-septal regions and to controls. No difference was seen between septal and non-septal regions of control patients (figure 4).

Determinants of T1 and myocardial strain

Results are shown in table 3. Global native T1 showed a significant negative correlation with body mass index (BMI) and a positive correlation with diastolic BP, as well as a non-significant trend with dialysis vintage. There was a significant correlation between global native T1 and GCS as well as global native T1 and GLS. There was also a significant correlation observed between septal native T1 and septal mid-ventricular systolic strain, with no correlation between non-septal native T1 and non-septal mid-ventricular systolic strain (figure 5). In a stepwise linear regression model that included BMI, diastolic and systolic BP, dialysis vintage, hemoglobin, hypertension and number of anti-hypertensive agents as predictors of global native T1, only BMI was an independent predictor (adj R^2 = 0.164, *F*-Statistic 7.482, *P*=0.01, Global T1 = 1334.4 + (-2.617 x BMI).

GLS was found to also correlate with LV mass index, LV end-diastolic volume index (LVEDVI), LVEF and past medical history of coronary artery disease. In a stepwise linear regression model that included LVEF, LVEDVI, history of coronary artery disease, hemoglobin, systolic BP, dialysis vintage, hypertension and number of anti-hypertensives as predictors of GLS, LVEF was the only independent predictor (adj R^2 = 0.268, *F*-Statistic 13.092, *P*=0.001, GLS = -1.709 + (-0.281 x LVEF). GCS also correlated with LVEF.

Discussion

Our results show, that native T1 time is significantly higher in patients with ESRD on HD than in control subjects, and this is associated with a global reduction in myocardial strain. We have also demonstrated for the first time significantly increased T1 signal in septal myocardium compared to non-septal segments in HD patients, a difference that was not present in control patient. This suggests levels of myocardial fibrosis may be highest in the interventricular septum of HD patients. Furthermore, we have shown for the first time that systolic strain is significantly reduced in septal myocardium compared to non-septal myocardium in HD patients, again a difference that was not present in control patients. Consistent with previous results we have confirmed abnormal GLS in HD patients compared to controls (14), but we additionally demonstrate impairment of GCS in HD patients compared to controls and that these markers of sub-clinical LV dysfunction are present even in patients with preserved EF.

Native T1 is related to water content of the relevant tissue. Although it has been shown to correlate well with biopsy proven fibrosis in diseases of pressure overload (20) we do not currently have histological confirmation that this is the case in HD patients; indeed low grade inflammation may increase native T1 (25). Furthermore, there is concern as to whether inter-compartmental fluid shifts affect native T1 signal and this warrants further investigation. We studied all patients on a non-dialysis day (and never during their long-break) to standardize fluid balance between patients but we cannot exclude the possibility of myocardial oedema from fluid shifts on native T1 values. Nevertheless, native T1 mapping has been shown to be a useful tool in the assessment of several other diseases including, acute myocardial infarction (26,27), amyloidosis (28), Fabry's disease (29), iron deposition (30), excessive lipid content (31), or valvular heart disease (19,20). It is unlikely that the above conditions would confound our results, as iron overload and high lipid content are known to reduce native T1 signal (32), no patient in the HD group had a history of amyloidosis or clinical features of Fabry's disease and there was no difference between the HD and control group in rates of coronary artery disease or previous myocardial infarction.

Wang et al recently reported a study of hemodialysis patients that showed native T1 times (using the MOLLI sequence) at 3T were comparable to the global T1 values we have presented (1273.4±41.7ms), but not significantly higher than controls (1253.1±71.6ms) (33). The control values quoted by Wang et al are significantly above the normal ranges for native T1 at 3T previously published (34) and they offer no explanation for this difference. The control values we found are similar to those previously published (34). One further study of patients with CKD (not on dialysis) by Edwards et al has looked at native T1 signal using the MOLLI sequence imaged at 1.5T (14). They measured native T1 values of the inter-ventricular septum at basal and mid-myocardial level, finding native T1 times significantly higher than matched controls and patients with hypertension. Direct comparison of absolute native T1 values between this study and the study by Edwards et al is not possible due to the different imaging platforms used (3T vs 1.5T). Additionally we have shown that 50% of HD patients show clear and discrete mid-wall increased T1 signal in a pattern very similar to that seen in patients with dilated cardiomyopathy using late gadolinium enhancement, which represents replacement fibrosis (35). A previous biopsy study in ESRD has shown that the extent of myocardial fibrosis is similar to that seen in non-ischaemic dilated cardiomyopathy (2). Consistent with this finding we have demonstrated that the HD patients have markedly increased LV volumes and reduced ejection fraction compared to controls, indicating that these patients are in the process of developing dilated cardiomyopathy and in fact 10 of the patients already had significantly impaired ejection fraction (<50%).

In patients with cardiac disease, GLS is a significantly better predictor of all-cause mortality (36) and major adverse cardiac events (37) than EF. As systolic strain appears to be an early marker of systolic dysfunction in patients with CKD and ESRD, integrating its assessment into routine clinical care may allow earlier optimization of modifiable cardiac risk factors. The correlation shown between Native T1 and strain suggest that myocardial fibrosis causes impairment of systolic strain and is in keeping with findings that have correlated segmental

systolic strain and segmental native T1 values in patients with hypertension (11). Similar to previous work in CKD patients, we found a weak non-significant correlation between LV mass index and strain or native T1 signal in HD patients (14). Progression of LV hypertrophy and development of myocardial fibrosis are likely to occur as a continuum in patients with CKD and ESRD, with cellular regression, apoptosis, programmed cell death and myocyte necrosis occurring as levels of fibrosis increase. Moreover, as fibrosis increases, the burden of small vessel ischemia from disruption of capillary beds is likely to exacerbate these problems further, hastening the development of fibrosis. However, as in other cardiac conditions, the degree of left ventricular hypertrophy and myocardial fibrosis are not predictable based on haemodynamic load (38). This means that complementary information may be obtained from LV mass and native T1 measurements.

The correlation between native T1 and BMI may be partly explained by the phenomenon of reverse epidemiology seen in HD patients (39,40), where higher BMI's are associated with improved outcomes. Further studies are required to investigate possible mechanisms that may underpin this association, including associations between native T1 and components of the malnutrition, inflammation, atherosclerosis syndrome. However this finding could simply be a Type I statistical error and should be viewed as hypothesis generating only.

The HD and control groups were well matched for demographics and co-morbidities, with the differences between groups being unlikely to bias the results we have shown. The control group were significantly older than the HD group and had significantly higher systolic BP. Age has been shown not to correlate with native T1 signal (34) and hypertensive patients are known to have increased native T1 (11), so if anything these differences would have diminished the chance of detecting differences between the groups. Despite significantly lower systolic BP, however, there were a higher percentage of patients in the HD group with a history of hypertension and this group were consequently on more anti-hypertensive agents. This difference was as anticipated, and while activation of the renin-angiotensin-aldosterone system is known to be involved in the

pathogenesis of cardiac fibrosis in uremic patients, it is certainly not the only factor that drives myocardial fibrosis development in HD patients (6,41-43). Eleven of the 22 control patients were found to be hypertensive (defined as BP> 140/90mmHg) despite having no history of hypertension, which was previously undiagnosed, but it would have been ideal to have had a matched-control group with essential hypertension. Mean hemoglobin was significantly lower in the HD group, but within target guidelines for HD patients and did not correlate significantly with native T1 value in either HD or control patients.

Limitations

This study is limited by its cross-sectional design. Subjects did not undergo coronary angiography to exclude epicardial coronary artery disease and we cannot, therefore, exclude ischemia from contributing to the native T1 values seen. This study does not address pathophysiological mechanisms for the development of fibrosis in ESRD and future studies should examine associations between serum and urine biomarkers of cardiac disease, myocardial fibrosis, native T1 values and strain. Histopathological studies are needed to assess whether quantitative and visual assessment of global and segmental native T1 correlates with actual myocardial fibrosis content and type in HD patients and whether T1 is linked to prognosis.

Conclusions

Native T1 times are significantly higher and systolic strain is significantly reduced in HD patients compared to controls. Native T1 times are highest and strain values are most impaired in the interventricular septum. Further studies are required to assess any contribution of myocardial oedema to native T1 times and assess the correlation between native T1 and histological fibrosis in the HD population.

Methods

The scans of 35 HD patients from the CYCLE-HD trial (ISRCTN 11299707) were analyzed and compared to the scans of 22 asymptomatic control patients from the PRIMID study (NCT01658345) (44). Control subjects were not known to have pre-existing cardiac disease but included those with common comorbidities (e.g. Hypertension, diabetes) so that the effect of CKD and HD could be assessed. Inclusion and exclusion criteria are shown in table 4. Demographic data, medical comorbidity, dialysis vintage, hematological and biochemical data were collected prospectively. Local research and ethics committee gave approval to all studies and written informed consent was obtained from all participants prior to recruitment.

Cardiac MRI Protocol

Patients were imaged on a 3 Tesla (3T) CMR platform (Skyra, Siemens Medical Imaging, Erlangen, Germany) using an 18-channel phased-array anterior coil due to the better signal intensity and limits of agreement of myocardial blood flow with microspheres compared to 1.5T with similar LV function analysis. Dialysis patients were all scanned on non-dialysis days, but not after the long-break, so all scans were conducted between 18 and 24 hours of most recent dialysis. The CMR protocols for acquiring cine imaging and native T1 maps were as previously described, (44), and conforming to internationally recognized standards (45). T1 data were acquired using a free-breathing with motion correction(MOCO), end-expiratory, ECG-gated single-shot modified look-locker inversion recovery (MOLLI) sequence (46), with the 3(3)3(3)5 sampling pattern, and the following typical parameters: slice thickness 8 mm, field of view 300 × 400 mm, flip angle 508, minimum TI 120 ms, inversion-time increment 80 ms. MOLLI maps of the left ventricle were acquired at the mid short-axis. The MOLLI sequence was chosen due to the techniques excellent inter and intra-observer variability at 3T (34) and because of local expertise (12). To minimize artefacts, acquisition was performed with the region of interest at isocentre, a small shim volume was applied around the myocardium, a large field of view (≥400 mm) was used, and imaging was repeated after changing the phase-encode direction or resonance offset frequency if artefacts persisted.

Electrographic gated breath-hold steady-state free procession (SSFP) long-axis cine images in 2, 3 and 4 chamber views were acquired. Short axis cine images covering the entire left ventricle were taken at 8 mm slice thickness, no gap, field of view 28 x 30 cm, matrix 208 x 256, repetition time 2.9 ms, echo time 1.2 ms, flip angle 64-79^0, temporal resolution <50ms, 80% phase, with 30 phases per cardiac cycle, in-plane image resolution 1.1 x 1.5 mm to 1.3 x 1.7 mm.

Cardiac MRI Scan Analysis

CMR scans were analyzed using the software package CMR^{42} (Circle Cardiovascular Imaging, Calgary, Alberta, Canada). All scans were analyzed offline by a single blinded observer. Image quality was assessed as being excellent, good, acceptable or poor. LV volumes and mass were quantified as previously described with (47) epicardial and endocardial contours of a contiguous stack of multiphase ventricular short axis cines (10-12 slices) at end-diastole and end-systole. The native T1 parametric map derived from MOCO MOLLI images was used to assess native T1 signal due to superior intra and inter-observer variability as described by our group compared to analyzing the MOCO series (12). Using the CMR^{42} T1 characterization module, endocardial and epicardial borders were drawn on MOCO MOLLI images for each patient, excluding epicardial fat, trabeculation and blood pool to give mean global T1 signal. The anterior right ventricular insertion point was defined to automatically divide the mid-ventricular slice into the 6-segment American Heart Association model (figure 6). Segments with areas of artifact were excluded, and mean T1 value was calculated from the remaining segments in individual patients. The analysis software uses a three-parameter least-squares fitting technique, with heart rate (HR) correction, to generate the average T1 value for the whole of the myocardium.

Strain analysis was undertaken using CMR-derived myocardial feature tracking (FT) with the 'tissue tracking' software package from CMR^{42} (48). Tissue tracking analysis is an automated frame-to frame template matching software package that derives similar quantitative deformation parameters from routinely available SSFP cine sequences, without the need for time-consuming 'tagged'

images (48). GCS was assessed by drawing endo- and epicardial contours on the LV short-axis cines in end-diastole (figure 6). The software automatically propagated these borders across the cardiac cycle using a template matching algorithm. For each patient, the mid-ventricular slice of the LV stack was analyzed, along with the two slices above (mid-basal and basal slices) and the two slices below (mid-apical and apical slices), so a total of five slices covering the LV were analyzed in each patient. GLS was assessed by drawing endo- and epicardial contours on LV long-axis cine in end-diastole and defining LV base and apex. Septal mid-ventricular circumferential systolic strain was calculated as the mean of segments 5 and 6 (of the mid-ventricular LV slice) and non-septal mid-ventricular circumferential systolic strain was calculated as the mean of segments 1,2,3 and 4 (of the mid-ventricular LV slice).

Sample size justification

A studt by Edwards et al showed that native T1 values of patients with CKD were increased compared to controls by 3.2% (986±37ms vs 955±30ms) (14). It is reasonable to expect a larger difference between native T1 values for HD and control patients. To show a 4% difference between native T1 of HD and control patients, based on the mean and standard deviation from healthy control patients imaged at 3T (1092.27±34.29ms) (12) with 95% power requires 17 patients in each group (α =0.05).

Statistical Analysis

Statistical analysis was undertaken using SPSS-22 software (Statistical Package for the Social Sciences, Chicago, IL, USA) and Graphpad Prism version 6.04 (GraphPad Software, Inc., La Jolla, CA, USA). Normality was assessed using the Shapiro–Wilk test, histograms, and Q–Q plots. Parametric data are expressed as mean ±standard deviation and non-parametric data are expressed as median (interquartile range). Patients and control values were compared by independent t-tests and Mann-Whitney U tests. Chi-squared tests and Fishers exact tests were used to assess for differences between nominal variables and are expressed as 'count' (%). A type 1 model 2-way ANOVA was used to assess for differences between non-septal and septal segmented T1 values in HD and control patients, with Sidak's multiple comparison tests used for post-hoc

analyses. Correlations between variables were assessed using Pearson's and Spearman's-rank analysis for normally and non-normally distributed data respectively. Stepwise multivariate linear regression models were used to assess for the independent influence of significant individual variables on T1 values and on strain.

Disclosure

None of the authors have any competing interests to declare, financial or otherwise.

References

(1) Mall G, Huther W, Schneider J, et al. Diffuse intermyocardiocytic fibrosis in uraemic patients. Nephrol Dial Transplant 1990;5(1):39-44.

(2) Aoki J, Ikari Y, Nakajima H, et al. Clinical and pathologic characteristics of dilated cardiomyopathy in hemodialysis patients. Kidney Int 2005;67(1):333-340.

(3) Diwan A, Wansapura J, Syed FM, et al. Nix-mediated apoptosis links myocardial fibrosis, cardiac remodeling, and hypertrophy decompensation. Circulation 2008 Jan 22;117(3):396-404.

(4) Nishida K, Kyoi S, Yamaguchi O, et al. The role of autophagy in the heart. Cell Death & Differentiation 2009;16(1):31-38.

(5) Ritz E. Left ventricular hypertrophy in renal disease: beyond preload and afterload. Kidney Int 2009;75(8):771-773.

(6) NON-CORONARY HEART DISEASE IN DIALYSIS PATIENTS: Hypertrophy and Fibrosis in the Cardiomyopathy of Uremia—Beyond Coronary Heart Disease. Seminars in dialysis: Wiley Online Library; 2008.

(7) HYPERTENSION IN HEMODIALYSIS PATIENTS: Cardiac Consequences of Hypertension in Hemodialysis Patients. Seminars in dialysis: Wiley Online Library; 2004.

(8) Ritz E, Wanner C. The challenge of sudden death in dialysis patients. Clin J Am Soc Nephrol 2008 May;3(3):920-929.

(9) Glassock RJ, Pecoits-Filho R, Barberato SH. Left ventricular mass in chronic kidney disease and ESRD. Clin J Am Soc Nephrol 2009 Dec;4 Suppl 1:S79-91.

(10) Shah AM, Solomon SD. Myocardial deformation imaging: current status and future directions. Circulation 2012 Jan 17;125(2):e244-8.

(11) Kuruvilla S, Janardhanan R, Antkowiak P, et al. Increased extracellular volume and altered mechanics are associated with LVH in hypertensive heart disease, not hypertension alone. JACC: Cardiovascular Imaging 2015;8(2):172-180.

(12) Singh A, Horsfield MA, Bekele S, et al. Myocardial T1 and extracellular volume fraction measurement in asymptomatic patients with aortic stenosis: reproducibility and comparison with age-matched controls. Eur Heart J Cardiovasc Imaging 2015 Jul;16(7):763-770.

(13) Urheim S, Edvardsen T, Torp H, et al. Myocardial strain by Doppler echocardiography. Validation of a new method to quantify regional myocardial function. Circulation 2000 Sep 5;102(10):1158-1164.

(14) Edwards NC, Moody WE, Yuan M, et al. Diffuse Interstitial Fibrosis and Myocardial Dysfunction in Early Chronic Kidney Disease. Am J Cardiol 2015;115(9):1311-1317.

(15) Liu YW, Su CT, Huang YY, et al. Left ventricular systolic strain in chronic kidney disease and hemodialysis patients. Am J Nephrol 2011;33(1):84-90.

(16) Odudu A, Eldehni MT, McCann GP, et al. Characterisation of cardiomyopathy by cardiac and aortic magnetic resonance in patients new to hemodialysis. Eur Radiol 2015:1-13.

(17) Mark P, Johnston N, Groenning B, et al. Redefinition of uremic cardiomyopathy by contrast-enhanced cardiac magnetic resonance imaging. Kidney Int 2006;69(10):1839-1845.

(18) Kribben A, Witzke O, Hillen U, et al. Nephrogenic systemic fibrosis: pathogenesis, diagnosis, and therapy. J Am Coll Cardiol 2009;53(18):1621-1628.

(19) Flett AS, Sado DM, Quarta G, et al. Diffuse myocardial fibrosis in severe aortic stenosis: an equilibrium contrast cardiovascular magnetic resonance study. Eur Heart J Cardiovasc Imaging 2012 Oct;13(10):819-826.

(20) Bull S, White SK, Piechnik SK, et al. Human non-contrast T1 values and correlation with histology in diffuse fibrosis. Heart 2013 Jul;99(13):932-937.

(21) Hinojar R, Varma N, Child N, et al. T1 Mapping in Discrimination of Hypertrophic Phenotypes: Hypertensive Heart Disease and Hypertrophic Cardiomyopathy: Findings From the International T1 Multicenter Cardiovascular Magnetic Resonance Study. Circ Cardiovasc Imaging 2015 Dec;8(12):10.1161/CIRCIMAGING.115.003285.

(22) Graham-Brown MP, Burton JO, McCann GP. The use of T1 mapping to define myocardial fibrosis in haemodialysis patients. Eur Heart J Cardiovasc Imaging 2016 Apr 13.

(23) Kali A, Cokic I, Tang RL, et al. Determination of location, size, and transmurality of chronic myocardial infarction without exogenous contrast media by using cardiac magnetic resonance imaging at 3 T. Circ Cardiovasc Imaging 2014 May;7(3):471-481.

(24) Dall'Armellina E, Ferreira VM, Kharbanda RK, et al. Diagnostic value of pre-contrast T1 mapping in acute and chronic myocardial infarction. JACC: Cardiovascular Imaging 2013;6(6):739-742.

(25) Hinojar R, Foote L, Ucar EA, et al. Native T1 in discrimination of acute and convalescent stages in patients with clinical diagnosis of myocarditis: a proposed diagnostic algorithm using CMR. JACC: Cardiovascular Imaging 2015;8(1):37-46.

(26) Messroghli DR, Niendorf T, Schulz-Menger J, et al. T1 mapping in patients with acute myocardial infarction: myocardial infarction and scar. J Cardiovasc Magn Reson 2003;5(2):353-359.

(27) Ugander M, Bagi PS, Oki AJ, et al. Myocardial edema as detected by pre-contrast T1 and T2 CMR delineates area at risk associated with acute myocardial infarction. JACC: Cardiovascular Imaging 2012;5(6):596-603.

(28) Karamitsos TD, Piechnik SK, Banypersad SM, et al. Noncontrast T1 mapping for the diagnosis of cardiac amyloidosis. JACC: Cardiovascular Imaging 2013;6(4):488-497.

(29) Pica S, Sado DM, Maestrini V, et al. Reproducibility of native myocardial T1 mapping in the assessment of Fabry disease and its role in early detection of cardiac involvement by cardiovascular magnetic resonance. J Cardiovasc Magn Reson 2014 Dec 5;16:99-014-0099-4.

(30) Pedersen SF, Thrysoe SA, Robich MP, et al. Assessment of intramyocardial hemorrhage by T1-weighted cardiovascular magnetic resonance in reperfused acute myocardial infarction. J Cardiovasc Magn Reson 2012;14(59):22935462.

(31) Scholz TD, Fleagle SR, Parrish F, et al. Effect of tissue fat and water content on nuclear magnetic resonance relaxation times of cardiac and skeletal muscle. Magn Reson Imaging 1990;8(5):605-611.

(32) Germain P, El Ghannudi S, Jeung M, Ohlmann P, et al. Native T1 Mapping of the Heart–A Pictorial Review. Clinical Medicine Insights.Cardiology 2014;8(Suppl 4):1.

(33) Wang L, Yuan J, Zhang S, et al. Myocardial T1rho mapping of patients with end-stage renal disease and its comparison with T1 mapping and T2 mapping: A feasibility and reproducibility study. Journal of Magnetic Resonance Imaging 2016.

(34) Dabir D, Child N, Kalra A, et al. Reference values for healthy human myocardium using a T1 mapping methodology: results from the International T1 Multicenter cardiovascular magnetic resonance study. J Cardiovasc Magn Reson 2014;16(1):69.

(35) Assomull RG, Prasad SK, Lyne J, et al. Cardiovascular magnetic resonance, fibrosis, and prognosis in dilated cardiomyopathy. J Am Coll Cardiol 2006;48(10):1977-1985.

(36) Kalam K, Otahal P, Marwick TH. Prognostic implications of global LV dysfunction: a systematic review and meta-analysis of global longitudinal strain and ejection fraction. Heart 2014 Nov;100(21):1673-1680.

(37) Stanton T, Ingul CB, Hare JL, et al. Association of myocardial deformation with mortality independent of myocardial ischemia and left ventricular hypertrophy. JACC: Cardiovascular Imaging 2009;2(7):793-801.

(38) Dweck MR, Joshi S, Murigu T, et al. Left ventricular remodeling and hypertrophy in patients with aortic stenosis: insights from cardiovascular magnetic resonance. J Cardiovasc Magn Reson 2012;14(50):851.

(39) Kalantar-Zadeh K, Block G, Humphreys MH, Kopple JD. Reverse epidemiology of cardiovascular risk factors in maintenance dialysis patients. Kidney Int 2003;63(3):793-808.

(40) Kalantar-Zadeh K. Causes and consequences of the reverse epidemiology of body mass index in dialysis patients. Journal of renal nutrition 2005;15(1):142-147.

(41) Amann K, Simonaviciene A, Medwedewa T, et al. Blood pressure-independent additive effects of pharmacologic blockade of the renin-angiotensin and endothelin systems on progression in a low-renin model of renal damage. J Am Soc Nephrol 2001 Dec;12(12):2572-2584.

(42) Amann K, Ritz E, Wiest G, et al. A role of parathyroid hormone for the activation of cardiac fibroblasts in uremia. J Am Soc Nephrol 1994 Apr;4(10):1814-1819.

(43) Amann K, Ritz E. Cardiac disease in chronic uremia: pathophysiology. Adv Ren Replace Ther 1997;4:212-224.

(44) Singh A, Ford I, Greenwood JP, et al. Rationale and design of the PRognostic Importance of MIcrovascular Dysfunction in asymptomatic patients with Aortic Stenosis (PRIMID-AS): a multicentre observational study with blinded investigations. BMJ Open 2013 Dec 18;3(12):e004348-2013-004348.

(45) Kramer CM, Barkhausen J, Flamm SD, et al. Standardized cardiovascular magnetic resonance (CMR) protocols 2013 update. J Cardiovasc Magn Reson 2013;15(1):1.

(46) Messroghli DR, Radjenovic A, Kozerke S, et al. Modified Look-Locker inversion recovery (MOLLI) for high-resolution T1 mapping of the heart. Magnetic resonance in medicine 2004;52(1):141-146.

(47) Singh A, Steadman CD, Khan JN, et al. Intertechnique agreement and interstudy reproducibility of strain and diastolic strain rate at 1.5 and 3 tesla: A comparison of feature-tracking and tagging in patients with aortic stenosis. Journal of Magnetic Resonance Imaging 2015;41(4):1129-1137.

(48) Schuster A, Stahnke V, Unterberg-Buchwald C, et al. Cardiovascular magnetic resonance feature-tracking assessment of myocardial mechanics: Intervendor agreement and considerations regarding reproducibility. Clin Radiol 2015;70(9):989-998.

Acknowledgments

This study is independent research arising from a Clinician Scientist Award (Dr James Burton, CS-2013-13-014) supported by the NIHR, an NIHR grant to Dr Gerald McCann (NIHR-CDF 2014-07-045) and a grant from the Van Geest Foundation. This work is also supported by the NIHR Leicester Cardiovascular Biomedical Research Unit based at University Hospitals of Leicester.

The views expressed in this publication are those of the authors and not necessarily those of the National Health Service, the National Institute for Health Research or the Department of Health.

Figures and legends

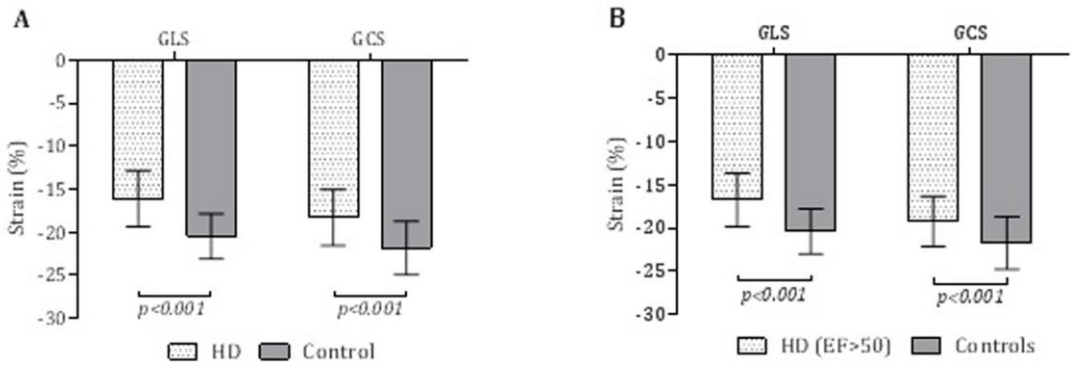

Figure 1: A: Comparison of GLS and GCS between HD patients and controls. **B:** Comparison of GLS and GCS between HD patients with preserved ejection fraction (>50%, n=25) and controls.

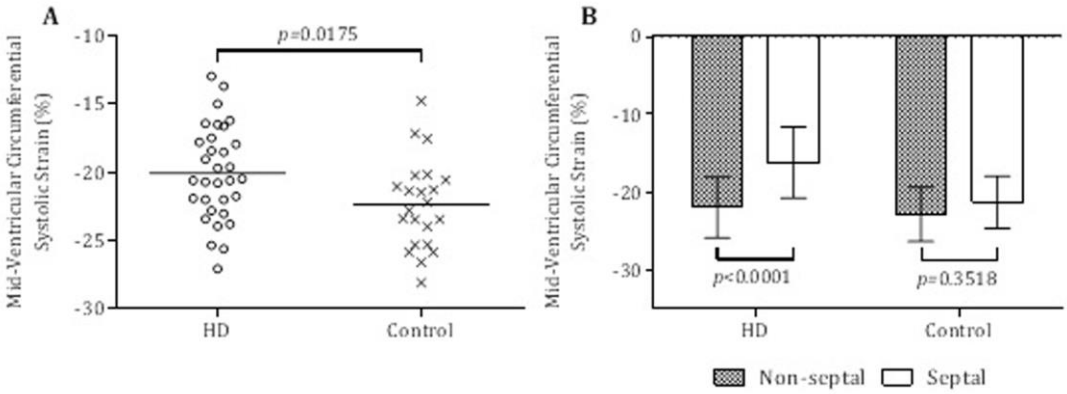

Figure 2: A: Mid-ventricular circumferential systolic strain of hemodialysis patients vs controls. **B:** Septal vs non-septal systolic strain of mid-ventricular slice for HD and control patients.

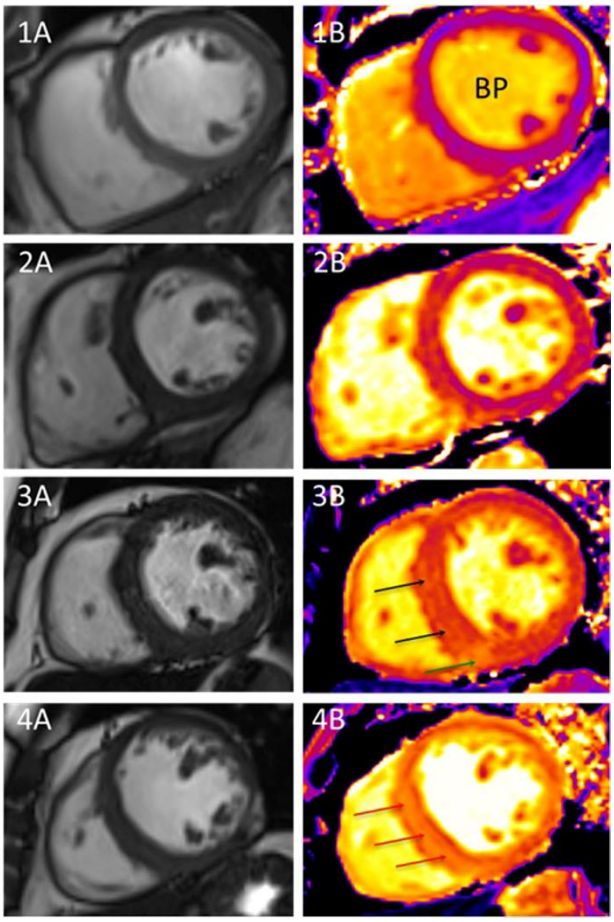

Figure 3: Examples of end diastolic cine images and corresponding T1 parametric maps in 1 control and 3 Hemodialysis patients

Illustrates how native T1 mapping may be able to differentiate diffuse interstitial fibrosis from replacement fibrosis in HD patients. Panels labeled 'A' show the end diastolic cine MRI slice of patients at mid-ventricular level. None of the cine slices demonstrate any abnormality of myocardial tissue. Panels labeled 'B' are the native T1 parametric maps at the same slice position in the same patients. As T1 times increase color coding changes from purple, to orange to yellow (blood pool; labelled BP). Panel 1 is of a 56 year old control patient. Mean global T1 is 1070ms, with no difference between septal and non-septal segments (1069ms vs 1072ms). Panel 2 shows a 71 year old HD patient with a 31 month dialysis vintage. Mean global T1 is significantly raised at 1238ms with a septal T1 of 1261ms and non-septal T1 of 1223ms. Visually there is no discrete area of enhancement. Panel 3 is of a 58 year old male HD patient of 46 month dialysis vintage. Mean global T1 is raised further at 1287ms, with septal T1 of 1312ms and non-septal T1 of 1255ms. Black arrows show discrete mid-wall inter-ventricular scarring (yellow), whilst the green arrow shows increased signal at the junction of the inferior insertion point to the septum . Panel 4 is of a 60 year old male HD patient of 48 month dialysis vintage with highest mean global T1 is 1368ms, with non-septal T1 of 1343 and septal T1 of 1387. There is discrete mid-wall of interventricular septum stripe that is clearly visible and likely represents irreversible, replacement fibrosis (23) (red arrows).

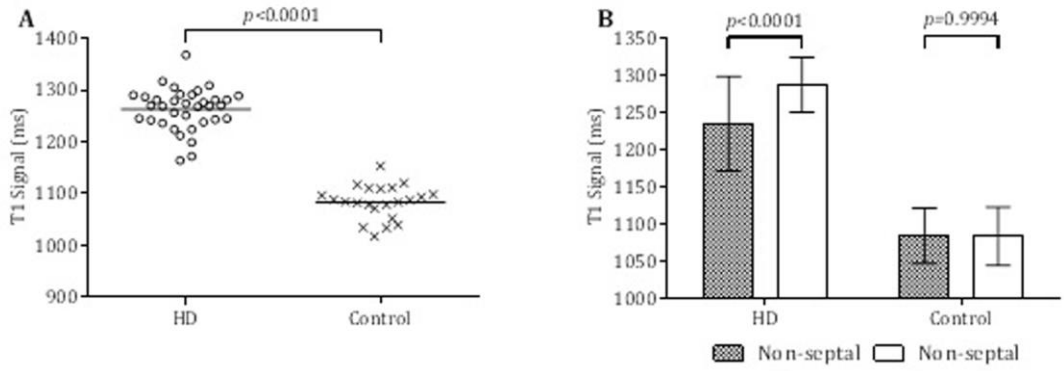

Figure 4: A: Mean native circumferential T1 in HD group and controls. **B:** Mean septal vs non-septal native T1 values in HD patients and control patients.

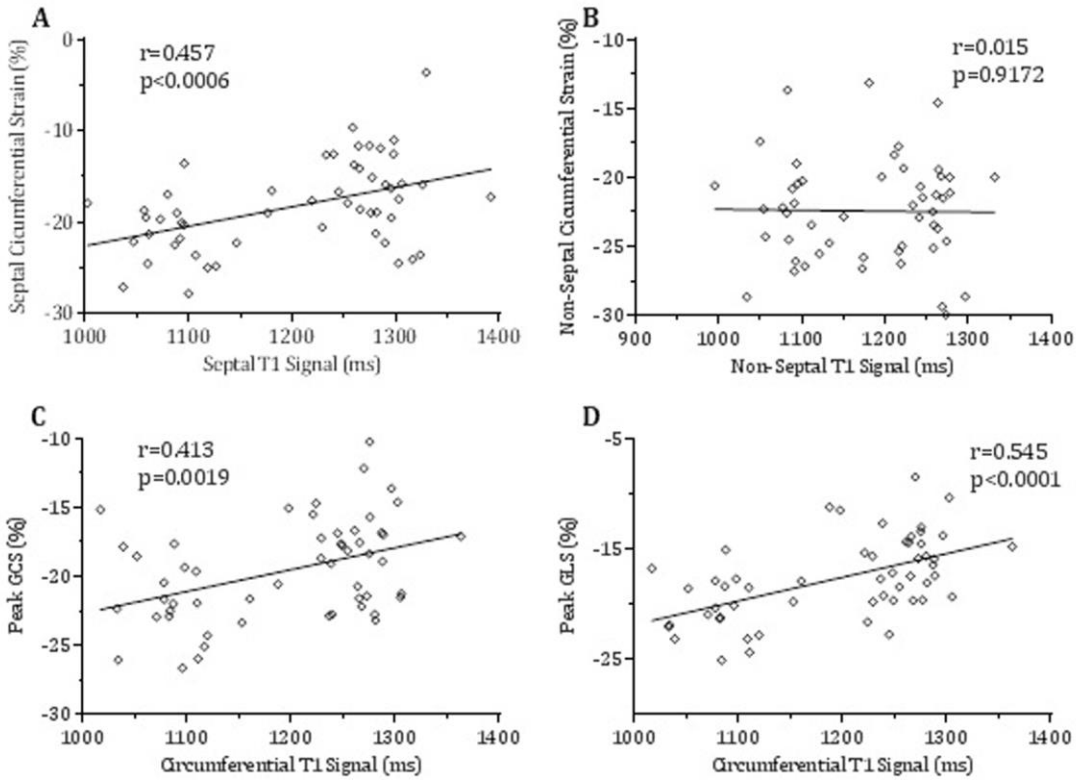

Figure 5: Correlations between: **A:** Septal mid-ventricular native T1 and septal mid-ventricular systolic strain. **B:** Non-septal mid-ventricular native T1 and non-septal mid-ventricular systolic strain **C:** Global native T1 and peak global circumferential strain (GCS) **D:** Global native T1 signal and peal global longitudinal strain (GLS).

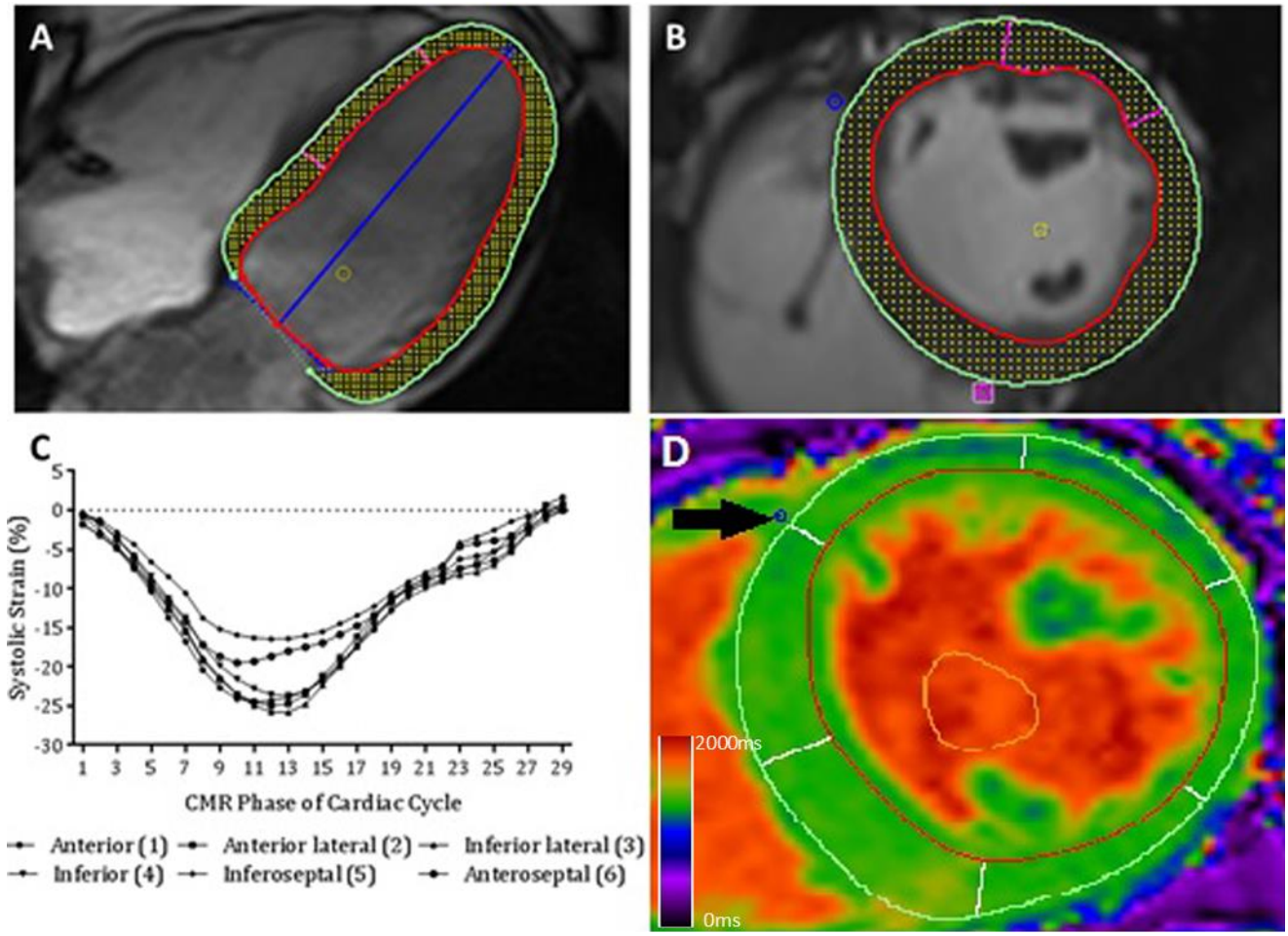

Figure 6: Analysis with software package CMR[42]. Endocardial and epicardial contouring in end-diastole for systolic strain analysis in long axis (**A**) and short axis (**B**). Segmental strain curves for each myocardial segment (**C**). Circumferential and segmental native T1 assessment using CMR[42] software on native T1 parametric map (**D**). Segments are calculated from defining the RV insertion point (arrow).

Tables

Table 1: Demographic details of HD and control patients

Variable	HD *n*=35	Control *n*=22
Age (years)*	58 (40-69)	66 (60-76)
Male (n,%)	28, 80%	15, 68%
BMI (kg/m^2)	26 (23-31)	26 (25-28)
BSA (m^2)	1.92 (1.69-2.15)	1.91 (1.86-2.05)
Dialysis Vintage (months)	21 (11-60)	-
Haemoglobin (g/L)*	109 (97-123)	139 (133-152)
HbA1c(%)	5.41 ± 1.7	6.1 ± 0.7
SBP (mmHg)*	139 ± 27	154 ± 25
DBP (mmHg)	77 ± 16	82 ± 9
HR (bpm)	75 ± 11	73 ± 8
Past medical and drug history		
Hypertension (n,%)*	26 (74.3%)	6 (27.3%)
Diabetes (n,%)	8 (22.9%)	2 (9.1%)
CAD (n,%)	9 (25.7%)	8 (36.4%)
Prev MI (n,%)	3 (8.6%)	0 (0%)
PVD (n, %)	1 (2.9%)	0 (0%)
ACEi (n,%)	6 (17.1%)	4 (18.2%)
ARB (n%)	3 (8.6%)	1 (4.5%)
Diuretic (n,%)	5 (14.3%)	2 (9.1%)
Beta Blocker (n,%)*	13 (37.1%)	1 (5.4%)
Statin (n,%)	13 (37.1%)	10 (45.5%)
Calcium Channel Blocker (n,%)	11 (31.4%)	4 (18.2%)
Number of antihypertensives*	1.06±1.03	0.5±0.913

Mean values with SD expressed as n ±SD. Median values are expressed as n (lower and upper quartiles). N, % = Chi-squared + %. *Values show significant difference between groups, P<0.05

Table 2: Comparison of native circumferential and segmental native T1 map, GCS, and GLS left ventricular function volumes and masses between HD and control patients.

Variable	HD *n*=35 [missing values]	Control *n*=22 [missing values]	*P* Value
LVMI (g/m^2)	55.7 (46.9-64.4)	42.1 (39.4-48.6)	<0.001
LVEDVI (ml/m^2)	105.2 (78-118.1)	76.8 (69.8-85.2)	0.002
LVESVI (ml/m^2)	50.2 (35.9-59.6)	30.4 (28-35.1)	<0.001
LVEF (%)	51.9 (49.1-55.9)	59.5 (56.8-61.2)	<0.001
LVM/LVEDV (g/mL)	0.56 (0.5-0.69)	0.56 (0.53-0.63)	0.961
GLS (%)	-16.1±3.3 [2]	-20.4±2.6	<0.001
GCS (%)	-18.3±3.3 [2]	-21.7±3.1	<0.001
Mid-ventricular septal systolic (%)	-16.2±4.6	-21.3±3.4	<0.001
Mid-ventricular non-septal systolic strain (%)	-21.9±3.9	-22.9±3.5	0.67
Mid-ventricular global T1 (ms)	1269.51 (1241.72-1289.01)	1085.2 (1066-1109.2)	<0.001
Mid-ventricular septal T1 (ms)	1292.7 (1258.9-1310.4)	1088.8 (1059.7-1103.5)	<0.001
Mid-ventricular non-septal T1 (ms)	1252.3 (1219.2-1269.6)	1090.8 (1066.5-1102.2)	<0.001

Mean values with SD expressed as n ±SD. Median values are expressed as n (lower and upper quartiles). [] = missing data from segments. GCS, global circumferential strain; GLS, global longitudinal strain; LVEF, left ventricular ejection fraction; LVEDVI, left ventricular end-diastolic volume index; LVESVI, left ventricular end-systolic volume index; LVMI, left ventricular mass index; ms, milliseconds.

Table 3: Correlation coefficients of global native T1 values GCS and GLS to potential determinants in HD patients.

CMR Parameter	Native Global T1		GLS		GCS	
	r-value	*P* value	r-value	*P* value	r-value	*P* value
Native Global T1	--	--	0.545	<0.001	0.413	0.002
LVMI	0.25	0.15	0.31	0.08	-0.33	0.13
LVEDVI	0.24	0.16	0.46	0.006	0.11	0.54
LVESVI	0.18	0.31	0.16	0.35	-0.12	0.5
LVEF	-0.18	0.31	-0.54	0.001	-0.37	0.02
LVM/LVEDV	0.09	0.62	-0.12	0.5	-0.21	0.24
Age	0.19	0.28	0.22	0.21	0.03	0.85
Dialysis Vintage	0.32	0.065	0.147	0.41	0.05	0.76
BMI	-0.42	0.012	-0.13	0.46	-0.11	0.53
Systolic BP	0.22	0.20	0.13	0.46	0.06	0.75
Diastolic BP	0.35	0.04	0.09	0.61	0.16	0.35
HbA1c	-0.48	0.83	-0.33	0.13	-0.2	0.36
PTH	0.27	0.14	0.06	0.73	-0.03	0.86
History of CAD	-0.12	0.50	-0.37	0.03	-0.13	0.46
History of HTN	-0.25	0.15	-0.27	0.13	-0.26	0.13

GCS, global circumferential strain; GLS, global longitudinal strain; LVEF, left ventricular ejection fraction; LVMI, left ventricular mass index; LVEDVI, left ventricular end-diastolic volume index; LVESVI, left ventricular end-systolic volume index; LVM/LVEDV, left ventricular mass / left ventricular end diastolic volume; BMI, body mass index; BP, blood pressure; PTH, parathyroid hormone; CAD, coronary artery disease; HTN, hypertension.

Table 4: Eligibility and Exclusion criteria

Eligibility Criteria	Exclusion Criteria
• Prevalent HD patient (>three months, dialysis patients only) • Aged 18 years or older • Able and willing to give informed consent • No acute illness	• unable to undergo MRI scanning (metal implants, severe claustrophobia) • Unable to give informed consent